



## 20 Myr of eccentricity paced lacustrine cycles in the Cenozoic Ebro Basin



Luis Valero<sup>a,\*</sup>, Miguel Garcés<sup>a</sup>, Lluís Cabrera<sup>a</sup>, Elisenda Costa<sup>b</sup>, Alberto Sáez<sup>a</sup>

<sup>a</sup> Institut de Recerca GEOMODELS, Departament d'Estratigrafia, Paleontologia i Geociències Marines, Facultat de Geologia, Universitat de Barcelona, Martí i Franquès s/n, 08028 Barcelona, Spain

<sup>b</sup> Departament de Geodinàmica i Geofísica, Facultat de Geologia, Universitat de Barcelona, Martí i Franquès s/n, 08028 Barcelona, Spain

### ARTICLE INFO

#### Article history:

Received 20 February 2014  
Received in revised form 26 September 2014

Accepted 3 October 2014  
Available online 29 October 2014  
Editor: G.M. Henderson

#### Keywords:

long term astronomical forcing  
Eocene  
Oligocene  
Miocene  
continental paleoenvironments  
Ebro Basin

### ABSTRACT

Long-period orbital forcing is a crucial component of the major global climate shifts during the Cenozoic as revealed in marine pelagic records. A complementary regional perspective of climate change can be assessed from internally drained lake basins, which are directly affected by insolation and precipitation balance. The Ebro Basin in northeastern Iberia embraces a 20 Myr long continuous sedimentary record where recurrent expansions and retractions of the central lacustrine system suggest periodic shifts of water balance due to orbital oscillations. In order to test climatic (orbital) forcing a key-piece of the basin, the Los Monegros lacustrine system, has been analyzed in detail. The cyclostratigraphic analysis points to orbital eccentricity as pacemaker of short to long-term lacustrine sequences, and reveals a correlation of maxima of the 100-kyr, 400-kyr and 2.4-Myr eccentricity cycles with periods of lake expansion. A magnetostratigraphy-based chronostratigraphy of the complete continental record allows further assessing long-period orbital forcing at basin scale, a view that challenges alternate scenarios where the stratigraphic architecture in foreland systems is preferably associated to tectonic processes. We conclude that while the location of lacustrine depocenters reacted to the long-term tectonic-driven accommodation changes, shorter wavelength oscillations of lake environments, still million-year scale, claims for a dominance of orbital forcing. We suggest a decoupling between (tectonic) supply-driven clastic sequences fed from basin margins and (climatic) base level-driven lacustrine sequences in active settings with medium to large sediment transfer systems.

© 2014 The Authors. Published by Elsevier B.V. This is an open access article under the CC BY-NC-ND license (<http://creativecommons.org/licenses/by-nc-nd/3.0/>).

### 1. Introduction

Astronomically-tuned oceanic sedimentary records show that certain rare orbital configurations were favorable to polar ice-sheet expansions, thus controlling global climate trends (Lourens and Hilgen, 1997). Internally drained basins may be particularly sensitive to climate change because lake-level oscillations readily account for the balance between precipitation and evaporation. Unfortunately, closed drainage conditions rarely persist for long because erosion and fluvial capture operate at shorter, million-year time-scales (García-Castellanos et al., 2003). Outstanding exceptions are found in Neogene to recent sediments of Lake Baikal (Kashiwaya et al., 2001) and the Triassic–Jurassic Rift System of Newark Supergroup of eastern North America (Olsen 1986; Olsen and Kent, 1999), where lacustrine sequences record long-period orbital forcing.

Assessing the climatic origin of large-scale sedimentary cycles is often controversial because internally driven geodynamic forces typically operate at  $10^6$ – $10^7$  yr time scales (Petersen et al., 2010), a range which overlaps with the known orbital cycles of the very long period eccentricity (0.97-Myr and 2.4-Myr) and obliquity amplitude (obliquity nodes at average 1.2-Myr) for the last 50 Ma. In the context of endorheic foreland systems causal relationships link the million-year scale clastic sequences with tectonic uplift and erosion along the margins. Plus, despite large sediment transfer systems have a buffer effect on supply-driven sequences (Castelltort and Van Den Driessche, 2003), the signature of high-amplitude long-wavelength tectonic pulses can be transmitted at long distances within the sedimentary basin as subsidence or/and supply-driven sequences (Paola et al., 1992; DeCelles and Giles, 1996).

The Paleogene–Neogene Ebro Basin in NE Spain is a peculiar case among the circum-Mediterranean foreland basins because plate convergence and collision sustained a land-locked basin configuration since its seaway closure in the Late Eocene (Costa et al., 2010) until its river capture in the middle–late

\* Corresponding author. Tel.: +34 934034888.

E-mail addresses: [luisvalero@ub.edu](mailto:luisvalero@ub.edu) (L. Valero), [mgarces@ub.edu](mailto:mgarces@ub.edu) (M. Garcés).

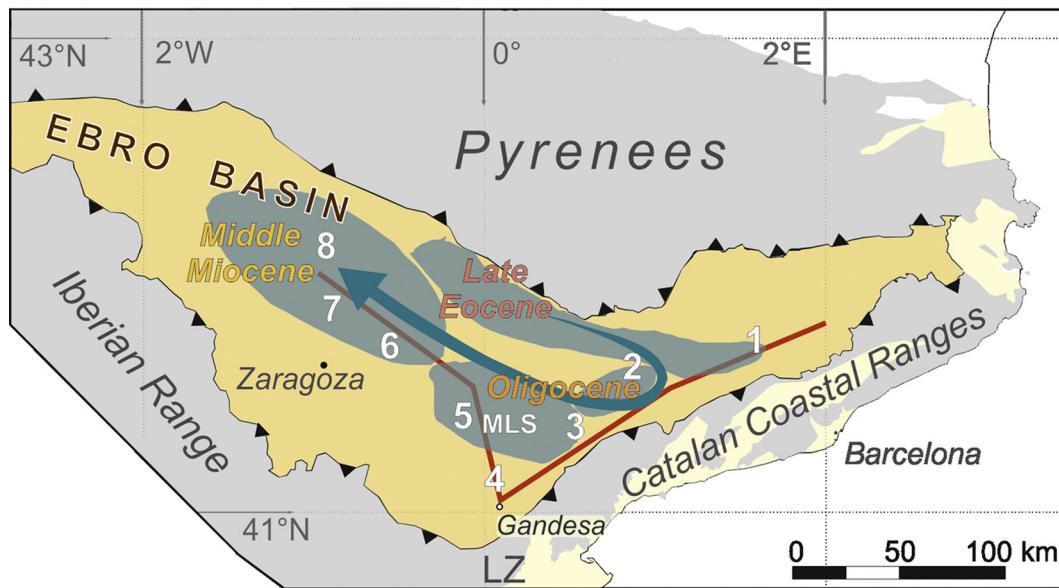


**Fig. 1.** Map of the Ebro Basin with location of lacustrine systems (blue-shaded areas) from late Eocene to Middle Miocene. Blue arrow marks the track of lacustrine shifting. Numbers indicate the location of sections discussed: 1. Mojà-Santpedor; 2. Rocafort-Sarral; 3. Tarrés-Cervià; 4. Gandesa-Bot; 5. Mina Pilar-Mequinenza; 6. Albalatillo-Lanaja; 7. San Caprasio; 8. Castejón-Sora. Red lines indicate the location chronostratigraphic panels of Fig. 8.

Miocene. The internally drained Ebro Basin underwent continuous and steady aggradation of terrigenous sediments fed from the active margins, grading into lacustrine sediments towards the inner basin areas. The progradational and retrogradational trends of the alluvial-lacustrine systems were used in the past for a chronostratigraphic subdivision based on the tectonosedimentary unit concept (Alonso-Zarza et al., 2002) or as tectonically-driven sequences (Anadón et al., 1989). The length and completeness of this record is most suitable for an independent, high-resolution magnetostratigraphic dating, which can provide a robust age model; a basic requirement for assessing the origin of sedimentary cycles.

In this paper we aim at exploring the tectonic and climatic (orbital) signatures in the recurrent expansion and retraction of the lake systems of the Eastern–Central Ebro Basin. To achieve this, a cyclostratigraphic study of the Late Oligocene–Early Miocene sequence of Los Monegros Lacustrine System (MLS) was carried out (Fig. 1). The MLS sequence is well suited for this study because the nearly three-dimensional outcrop exposures in the area of Mequinenza allow the precise identification of a thick (ca. 500 m) and continuous stack of successive lacustrine cycles. In addition, the magnetostratigraphy of these sequences can be used to construct an age model for astronomical tuning, as astronomical ages of geomagnetic reversals around the Oligocene–Miocene boundary are well constrained (Shackleton et al., 1999; Liebrand et al., 2011). To further test if the observed cyclicity is forced by long-period orbital oscillations, an integration of the complete late Eocene to middle Miocene succession of the Eastern and Central Ebro Basin is examined.

## 2. The Los Monegros Lacustrine System

The MLS sequence (Fig. 1, Supplementary Fig. A1) consists in shallow lacustrine limestone successions, grading laterally and vertically into mudflats and terminal lobes and small deltas formed by red mudstones and sandstones. The very low depositional gradient made this system very sensitive to water balance, where small changes of lake level affected large basin areas (Anadón et al., 1989; Arenas and Pardo, 1999; Sáez et al., 2007). Lake level changes (Fig. 2) controlled the sequential arrangement of the lacustrine and alluvial-lacustrine sedimentary units, which exhibit a hierarchical architecture. In the inner lacustrine sectors, within

the carbonate dominated successions, a basic 1.5 to 3 m thick (para)sequence occurs. This sequence displays a shallowing upwards trend, which includes from bottom to top: subaqueous coal deposits and/or calcisiltites (offshore facies), near-shore facies composed by gastropod and ostracode bearing micritic limestones and thin palustrine limestones overlain by greenish to gray mudstones (Cabrera and Sáez, 1987; Cabrera et al., 2002). The proportion of siliciclastic deposits (gray, variegated and red mudstones and sandstones) increases towards the marginal lacustrine zones, where thin limestone beds grade into red mudstones and thin sandstones.

The basic sequences can be grouped into 6–8 m thick carbonate dominated composite sequences in the lake depocenters. In the near-shore areas, composite sequences consist in 8–12 m thick mudstone dominated intervals with thin limestones interbedded. Carbonate-rich composite sequences are grouped into 25 to 35 m thick clusters, separated by thinner siliciclastic intervals which represent periods of major lake contraction. In its turn, in the mudstone dominated marginal lacustrine zones these clusters consist of limestone bed bundles interbedded with gray and variegated to red mudstone intervals. Finally, these clusters are grouped into thick limestone packages which correspond to the formal lithostratigraphic units of the Mequinenza and Torrente de Cinca carbonate-dominated units, and the alluvial Cuesta de Fraga Formation (Cabrera, 1983).

## 3. Magnetostratigraphy

A magnetostratigraphic study was carried out in order to provide an age model for the MLS sedimentary sequence. Two overlapping sections (PA and ME) were logged and later merged into a 307 m thick Mequinenza composite section (Fig. 3). Lithostratigraphic correlation between the PA and ME sections was feasible from field observations and later adjusted using magnetostratigraphic data (Fig. 3).

The Mequinenza section was sampled at 2 m stratigraphic intervals with a total number of 171 oriented paleomagnetic drill cores. Sampled lithologies included limestones, red to brown-grey silts and marls and, occasionally, fine-grained sandstones. Earlier magnetostratigraphic studies on the same stratigraphic units (Gomis et al., 1997; Barberà et al., 2001) showed that sediments retain

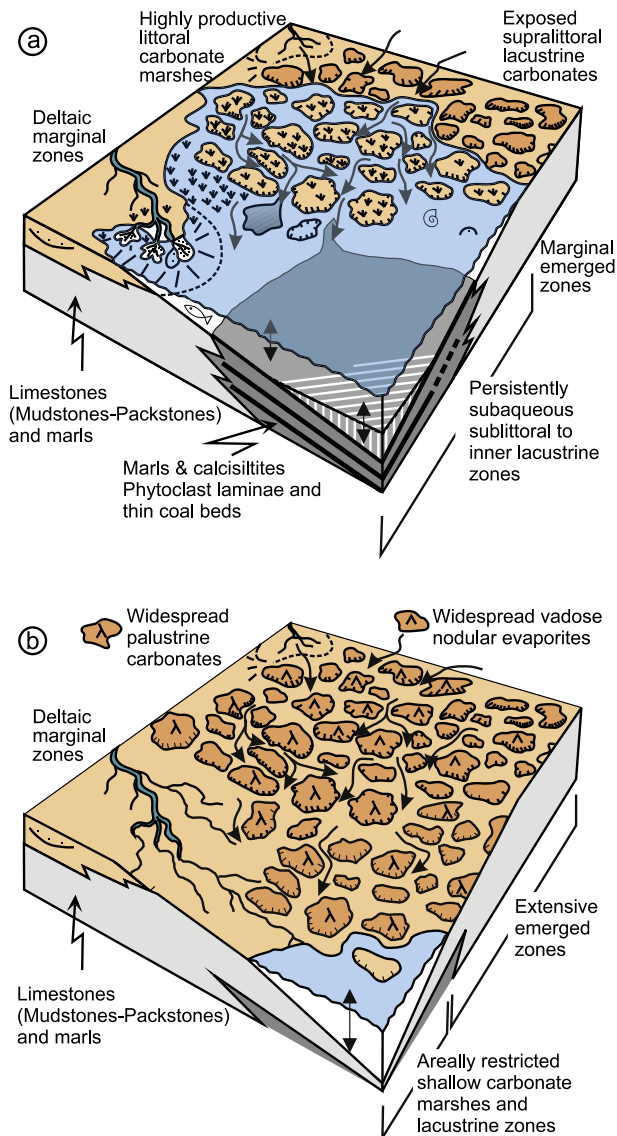


**Fig. 2.** Sedimentary model for the Mequinenza lacustrine sequences, modified after Cabrera et al. (2002). A) High-stand stage with coal deposits accumulated in the deepest parts. Laminated limestones grade into rooted mudstone, white, grey and greenish mudstone towards the lake margins. Red mudstone and sandstone occurred onshore. B) Low-stand stage with a detrital facies belt prograding basinwards.

a stable Characteristic Remanent Magnetization (ChRM) carried by either magnetite (limestones and marls) or hematite (red beds).

In order to isolate the ChRM, samples were stepwise thermally demagnetized at 50 °C temperature increments up to 300 °C and, thereafter at increments of 20 °C up to complete demagnetization of the NRM. Measurements were carried out in the laboratory of Paleomagnetism “Jaume Almera” (CCiTUB-CSIC) in Barcelona using a three axis superconducting rock magnetometer (2G-SRM750). Magnetic susceptibility was measured at each demagnetization step with a KLY-2 susceptibility bridge (Geofyzika Brno) in order to monitor mineralogical changes upon heating. The results from most of samples reveal the presence of two magnetic components (Fig. 4). A low-temperature, possibly viscous, component is removed after heating to 220 °C to 350 °C. Above this temperature a characteristic component is found with maximum unblocking temperatures ranging from 450 °C (limestones and grey silts) to 650 °C (red mudstones), interpreted as carried by the iron oxides magnetite and hematite, respectively. Substantial increases of magnetic

susceptibility often occurred upon heating to temperatures above 400 °C, thus possibly indicating the formation of magnetic minerals during demagnetization.

The ChRM components were picked after visual inspection of Zijderveld plots in 112 samples (65% of the total number of samples) and directions were calculated by means of principal components analysis (Kirschvink, 1980) (Fig. 4). Fisherian means of the normal and reversed polarity directions pass the reversal test, although the reversed polarity mean clearly presents an anomalous shallow inclination. This deviation from expected values could be explained as the result of partial overlap of a normal polarity viscous component. Both normal and reversed polarity means present a clockwise departure of 9.6° (normal) and 13.3° (reversal) from GAD. The large dispersion of directional data, however, does not give statistical significance to these differences.

The Virtual Geomagnetic Pole (VGP) latitude was calculated at sample level and plotted against thickness in order to establish a Local Magnetic Polarity Stratigraphy (Fig. 3), where magnetostratigraphic data from other sections in the region (Gomis et al., 1997; Barberà et al., 2001) (Fig. 5). The lower normal magnetozone in the Mequinenza section was consistently traced in the field and cross-checked with multiple magnetostratigraphic sections (Fig. 5), thus supporting a primary (syndimentary) origin of the magnetization. The base of this magnetozone is taken as the key horizon for correlation with the Mina Pilar section. Best match of the composite sequence with the GPTS confirms earlier calibration results (Barberà et al., 2001). Correlation of a short magnetozone in Mequinenza (N5 in Fig. 3) with Torrente de Cinca section further suggests the existence of a brief normal geomagnetic event within C6Cr (referred to as cryptochron C6r-1 in the CK95 GPTS, Cande and Kent, 1995). This short chron is also found in high resolution magnetostratigraphic records in deep sea sediments (Lanci et al., 2005), although not recognized in the most recent time scale compilations (Gradstein et al., 2004, 2012).

The resulting correlation allows constructing a robust age calibration of the MLS sequence extending between 28.5 Ma and 21.5 Ma (Fig. 5), placing the Oligocene–Miocene boundary near the base of the Torrente de Cinca Formation in this area. The average sedimentation derived from magnetostratigraphy reflects an overall trend of steadily decreasing rates, higher rates being recorded in lower units of Mina Pilar section (ca. 13 cm/kyr), and lower rates in the upper part of the Mequinenza section (ca. 6 cm/kyr). In addition to this regional trend, variations in sedimentation rate occur in relation to shifts in the sedimentary environment. As observed in the Miocene sequences of the central Ebro Basin (Pérez-Rivarés et al., 2004), lacustrine limestone units yielded accumulation rates (ca. 6 cm/kyr), lower than the average 9 cm/kyr of the distal alluvial redbed sediments of the Cuesta de Fraga Fm (Supplementary Fig. A2).

#### 4. Cyclostratigraphic analysis

Previous cyclostratigraphic analysis (Luzón et al., 2002; Barberà, 1999) revealed high frequency precession-related orbital forcing in specific limestone-dominated short intervals. But medium to low frequency (>100-kyr) cyclicity was undetermined because the studied time range were in all cases shorter than 1 Myr. In order to better examine the longer period cyclicity, a 500 m-thick composite sequence is studied here (Fig. 1, Fig. 3).

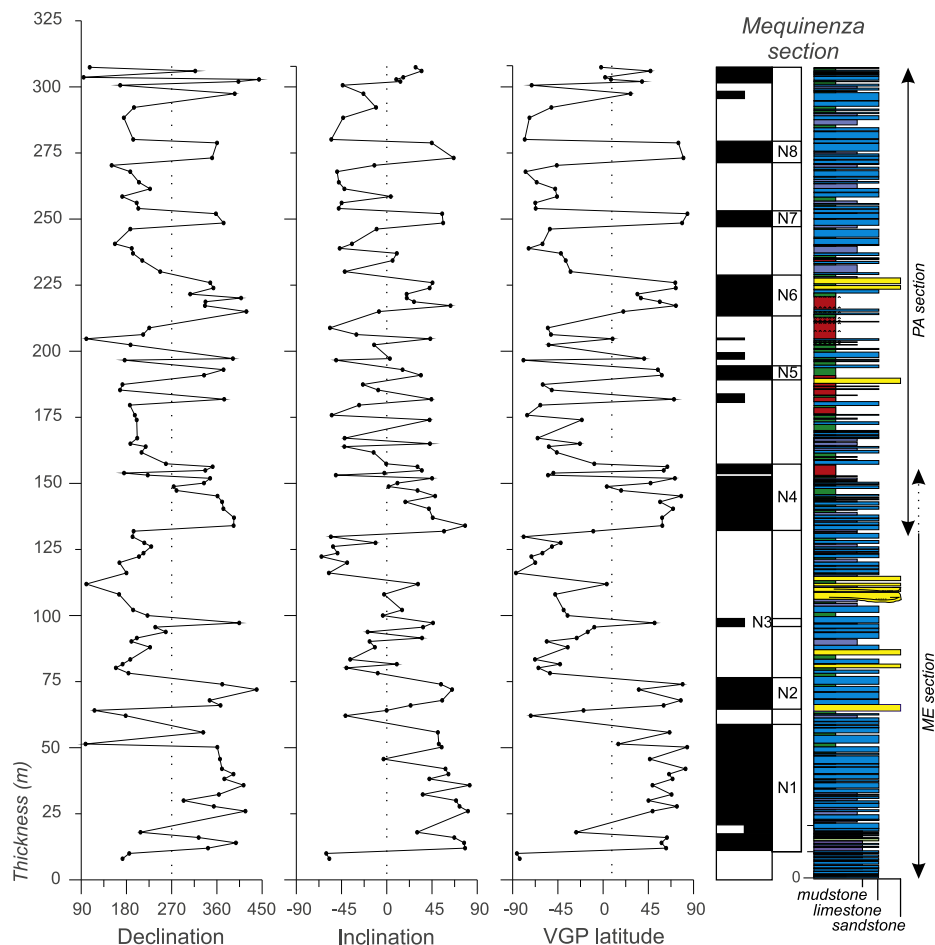


**Fig. 3.** Litho- and magnetostratigraphy of the Mequinenza composite section. (For interpretation of the references to color in this figure, the reader is referred to the web version of this article.)

#### 4.1. Depth rank

For the cyclostratigraphic analysis, a time series which represents relative lake-level oscillations was built on the basis of sedimentary facies. We assumed that shifting lacustrine facies responded basically to water-depth changes, these being controlled by climatically driven changes in the water budget (Freytet and Plaziat, 1982; Olsen and Kent, 1996, 1999; Luzón et al., 2002; Alonso-Zarza, 2003). A rank of facies which can be ordered from shallow to deep lake conditions was characterized, obtaining an inferred relative paleobathymetry for the lacustrine system (Olsen and Kent, 1996). To build a time series, depth values were taken through the section at constant stratigraphic intervals of 40 cm, corresponding to a time resolution of 4 to 7 kyr (described in detail in Supplementary Table A1 and Supplementary Material).

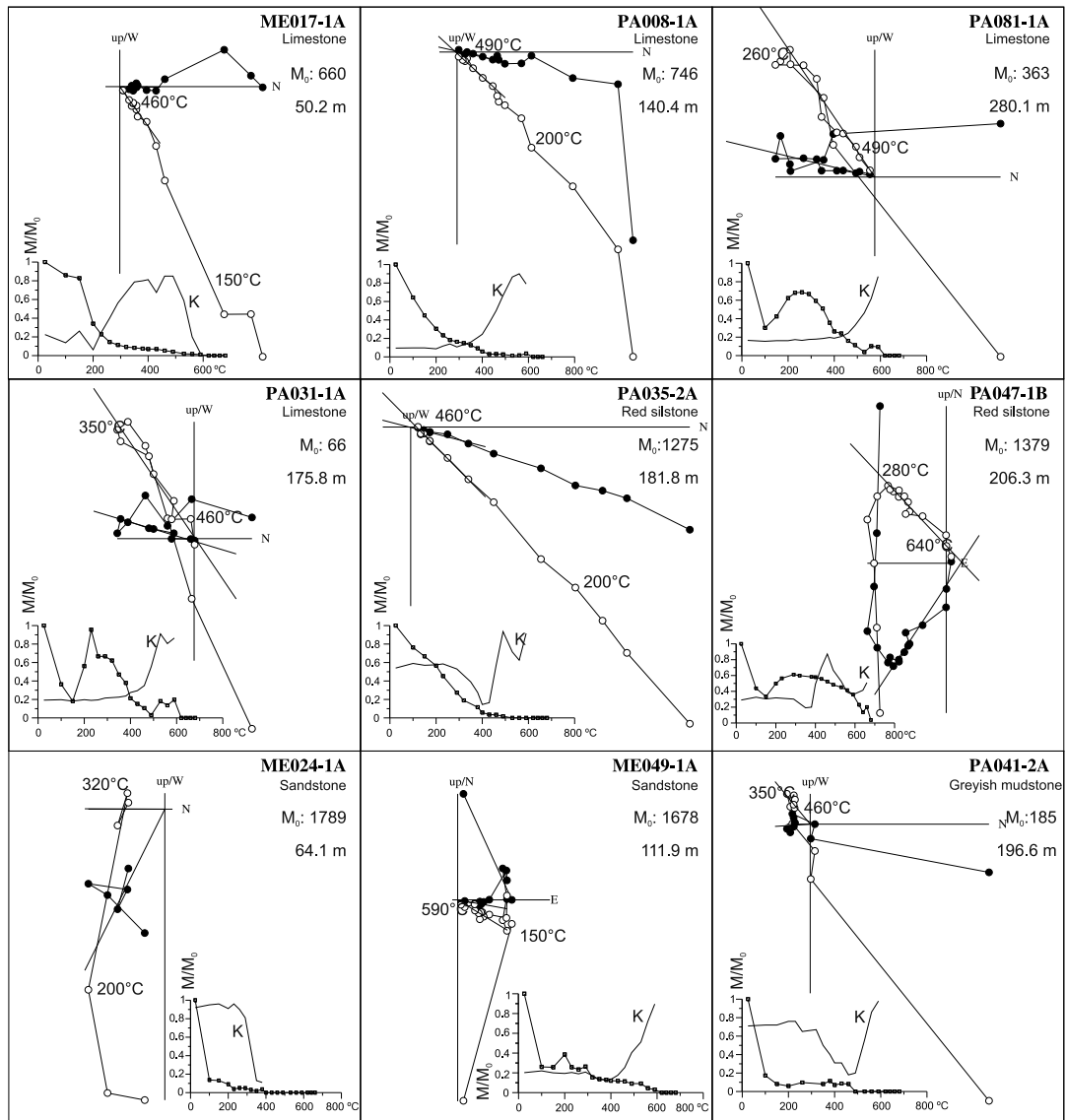
#### 4.2. Spectral analysis

Spectral analysis was done by REDFIT software (Schulz and Mudelsee, 2002) with a Rectangular/Blackman-Harris window and 2000 simulations. This method allowed estimating the red noise addition during data interpolation. Evolutionary wavelet spectra were obtained by the MATLAB script provided in Torrence and Compo (1998).

The MLS sequence encompasses several facies associations of varying clastic contribution which produced changes in sedimentation rate related to sedimentary environment, a source of noise in the spectral analysis (Machlus et al., 2008). To minimize distortions of the time series related to unsteady sedimentation, the sequence

was split into 6 intervals according to the lithology (Fig. 6). Spectral analysis in the depth (thickness) domain was carried out in all 6 intervals, yielding significant peaks at frequencies whose ratios reproduce the ratios of eccentricity of 400-kyr and 100-kyr, 41-kyr obliquity and precession (Table 1). A preliminary age model constrained by magnetostratigraphy confirms that the lower frequency and most ubiquitous spectral peak of 25–30 m yields an average period of 400-kyr (Fig. 7). Thus, the 400-kyr cycle was selected for tuning because of its stability, both in our data and in the astronomical solution. To facilitate this task, the 400-kyr cycle was isolated from higher frequency signals by applying a bandpass filter below 20 m (which would correspond to 334-kyr in the lowest sedimentation rate interval) (green curve in Fig. 6). The filtered signal reveals, superposed on the 400-kyr beat, a long-wavelength oscillation which we associate to the 2.4-Myr eccentricity cycle, with eccentricity maxima correlated to times of lake expansion and eccentricity minima to lake low-stands (Fig. 6).

Linkage of the time series with the 400-kyr term of the orbital eccentricity (Laskar et al., 2004) was completed with the Analyseries 2.0.4 software (Paillard et al., 1996). The 400-kyr cycle at the base of the Mequinenza section was found poorly represented in the filtered signal possibly because of an edge effect (the correlation between the Mequinenza and Mina Pilar sections represents a lateral shift of 5 km, Supplementary Material), but reasonably identifiable from the lithostratigraphic log. Two 400-kyr cycles at the top of the section are also obscured due to the lack of facies contrast at times of persistent high lake levels. Assuming the current astronomical calibration of the GPTS at the Oligocene–



Polarity	N	Dec	Inc	k	$\alpha_{95}$
Reverse	59	193.3	-25.1	4.4	10
Normal	53	9.6	49.8	4.6	10.3

Upper Hemisphere ○  
Lower Hemisphere ●

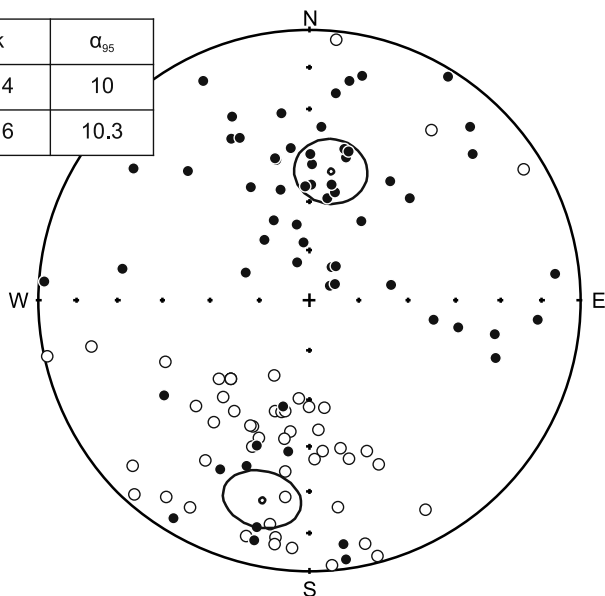


**Fig. 4.** Stepwise NRM thermal demagnetization (Zijderveld plots) of representative lithologies and normalized NRM and magnetic susceptibility changes upon heating.  $M_0$ : Initial NRM in  $10^{-6}$  A/m. Sample stratigraphic position in meters referred to Fig. 3. Below, stereonet projection of paleomagnetic directions and their associated normal and reversed mean directions.

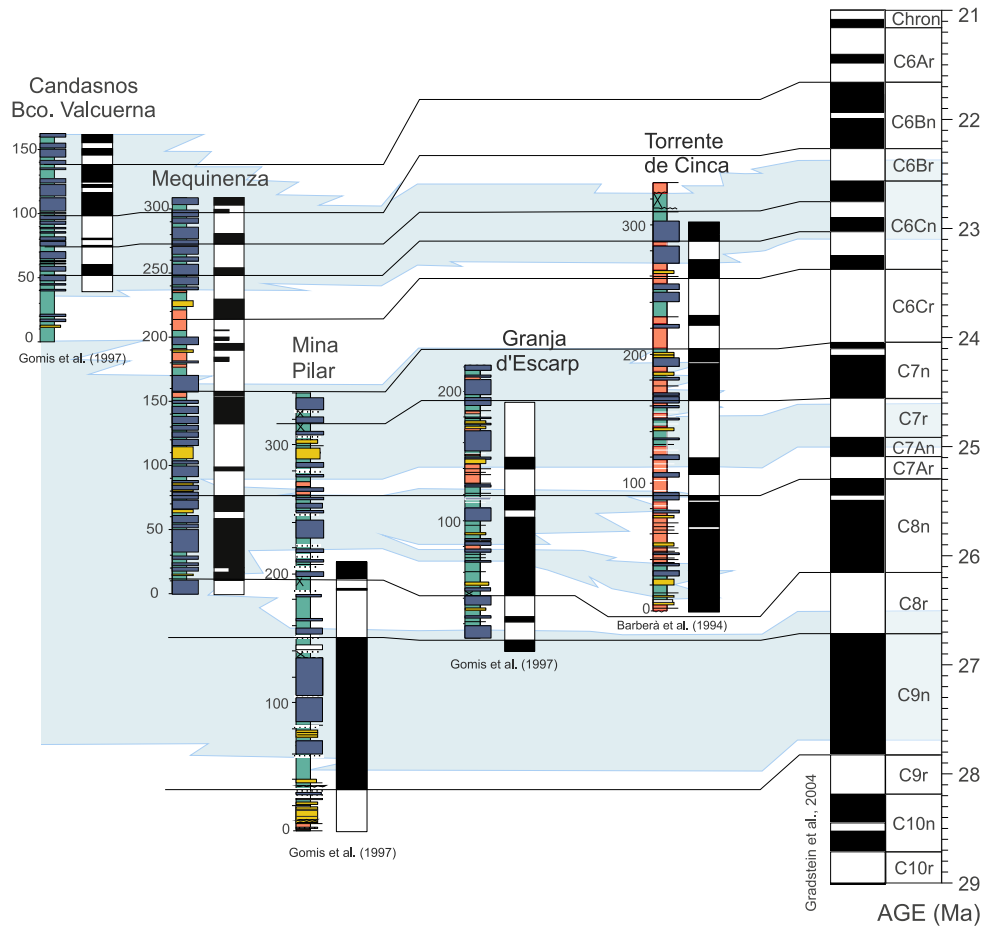


**Fig. 5.** Integrated magnetostratigraphy of the MLS sequence in the Mequinenza area based on earlier works (Gomis et al., 1997; Barberà et al., 2001) and the present study. Multiple overlapping magnetostratigraphic sections allow an identification of a sequence of reversals that can be traced laterally, thus giving strong evidence of a primary magnetization. The blue-shade bands mark the lacustrine facies.

**Table 1**  
Significant periodicities of paleobathymetry time series of the MLS sequence obtained from spectral analysis in depth domain (REDFIT software, Schulz and Mudelsee, 2002). The confidence of the peaks is shown with % of significance between brackets. The correspondence in time domain of each peak is calculated assumed a period of 405 kyr (interval MP2, ME1, ME2 and ME3) or 100 kyr (interval MP1 and MP3) for the longest cycle identified at each stratigraphic interval.

Section	Interval	405 (kyr)	100 (kyr)	41 (kyr)	23 (kyr)	19 (kyr)
Mequinenza	ME3	24.23 m (95%)	5.74 m (90%) 95.94 kyr	2.67 m (99%) 44.62 kyr		1.23 m (95%) 20.55 kyr
	ME2	28.79 m (99%)	7.03 m (95%) 98.89 kyr	3.55 m (90%) 49.93 kyr	1.66 m (95%) 23.35 kyr	1.379 m (95%) 19.39 kyr
	ME1	26.7 m (99%)	6.92 m (95%) 115.76 kyr	2.25 m (90%) 37.62 kyr	1.48 m (95%) 24.74 kyr	
Mina Pilar	MP3		10.40 m (90%) 31.15 kyr	3.24 m (90%) 31.15 kyr		
	MP2	28.35 m (95%)	7.73 m (90%) 110.42 kyr			1.31 m (95%) 18.71 kyr
	MP1		14.26 m (99%)			

Miocene transition (Shackleton et al., 1999; Liebrand et al., 2011; Gradstein et al., 2012), magnetic reversals bounding this age were taken as a constraint for tuning. The resulting time series was rescaled into age domain (red). A new spectral analysis of the resulting 400-kyr tuned time series revealed increasing power of the 100-kyr peak, and an alignment of the 100-kyr peaks in the evolutionary wavelet spectra (Fig. 7). These results allow to tune with the eccentricity solution (Laskar et al., 2004) after applying a band-pass filter centered at the 100-kyr (bandwidth 0.00165, blue filter in Fig. 6).

The new age model derived from astronomical tuning allows comparing ages of geomagnetic reversals with the recent calibrations of the time scale (Pälike et al., 2006; Gradstein et al., 2004, 2012). Agreement within the resolution of the eccentricity cycle is found with GTS2004 (Gradstein et al., 2004). On the contrary, a mismatch with GTS2012 (Gradstein et al., 2012) is noticed for ages older than 25 Ma, reaching a maximum discrepancy of 400 kyr at the base of chron C9n. Noteworthy the GTS2012, which for this interval relies on astronomical tuning (Gradstein et al., 2012), has an unsolved discrepancy of same order with the radiometric time scales (Gradstein et al., 2012).

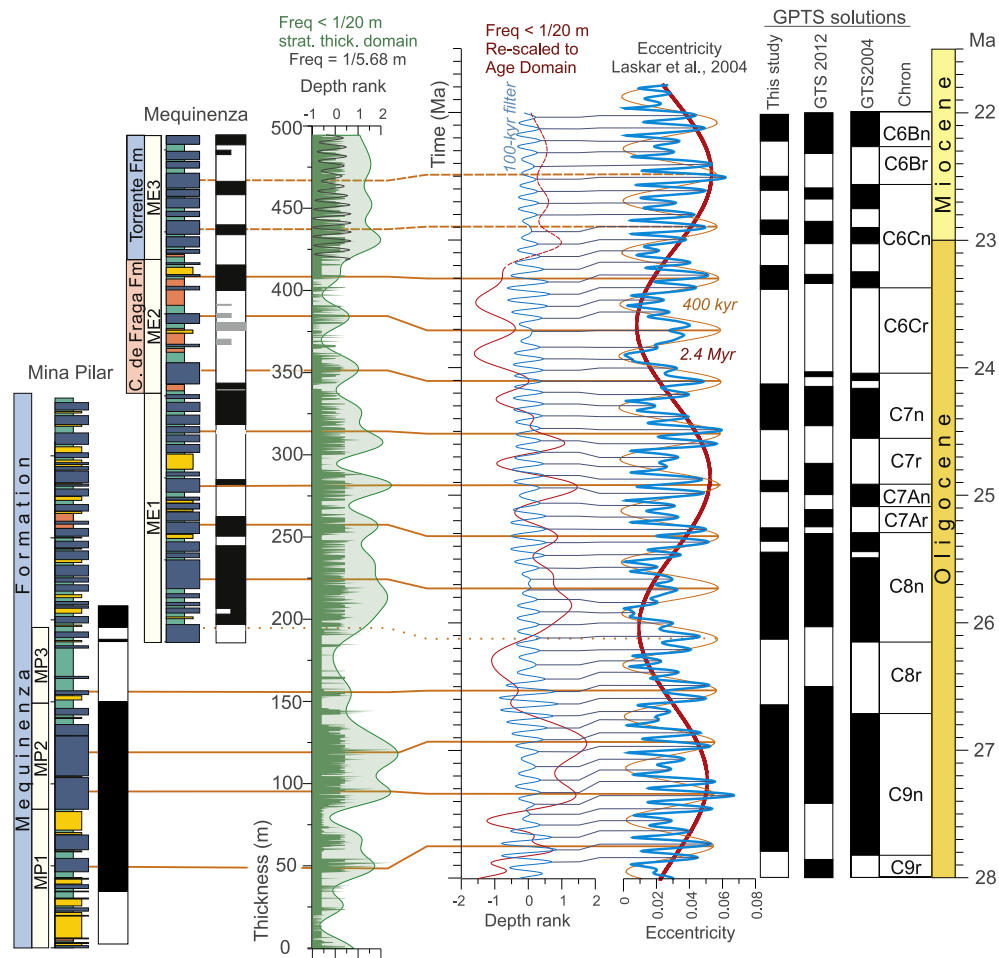


**Fig. 6.** Astrochronology of the MLS stratigraphic sequence. In the left, the stratigraphic logs are divided into 6 intervals according to the lithology. In green, the inferred bathymetry of the lake with an envelope which removes frequencies  $<20$  m. The filtered signal revealed a long-wavelength oscillation which is associated to the 2.4-Myr eccentricity cycle, where eccentricity maxima correlates to peaks of lake expansion. Superposed to this trend, a higher frequency signal is interpreted as the expression of the 400-kyr eccentricity cycle. Analysier software (Paillard et al., 1996) was used to link the filtered paleobathymetry series with the 400-kyr eccentricity cycle of the astronomical solution (Laskar et al., 2004). In the middle, the resulting time series was rescaled into age domain (red line) and a Gaussian filter centered at 100 kyr (bandwidth 0.00165) was applied. The output (blue) was linked to the 100-kyr eccentricity term of the astronomical solution. In the right, the age of geomagnetic reversals that results from this analysis is compared with most recent calibrations of the time scale (Gradstein et al., 2004, 2012).

## 5. Long-period orbital forcing of lacustrine sequences

The derived chronology of the MLS sequence reveals that three major phases of lacustrine expansion correlate to consecutive periods of maxima of the 2.4-Myr eccentricity cycle (Fig. 5, Fig. 6), thus suggesting long-period orbital forcing. Furthermore, the MLS sequence is integrated in a 20 Myr long sedimentary record which includes a succession of limestone formations representing shallow fresh-water perennial lakes. Some of these units extended over areas of up to 3000 km<sup>2</sup> at periods of lake high-stand (Anadón et al., 1989). Alternating with these relatively wet periods, nearly complete drying of the basin occurred at times of low-stand levels. A magnetostratigraphic framework is available for the complete sequence of the eastern and central Ebro Basin after the work of Barberà et al. (2001), Gomis et al. (1997), Costa et al. (2010, 2011) and Pérez-Rivarés et al. (2002, 2004). These studies provide a time framework to test long-period orbital forcing of lacustrine sedimentation in the Eastern Ebro Basin (Fig. 8).

Succeeding basin continentalization the earliest lacustrine units in the East Ebro Basin were deposited adjacent to the South-Pyrenean Front. A first phase of evaporite deposition was followed by the fresh-water lacustrine limestones of the Castelltallat Fm, which extended over 100 km along an E–W elongated belt and reached maximum thickness of 200 m at its depocenter. Magne-

tostratigraphy of the Santpedor-Moià composite section (Costa et al., 2011) allows a precise correlation of this phase of lacustrine expansion to the lower part of chron C13r (Fig. 8), while by the end of the Eocene lake environments shrink and practically disappeared from the eastern Ebro Basin. During this period, the E/O boundary is marked by a distinct progradation of an amalgamated sandstone unit, interpreted as the response of the fluvial fan system to a transient lake level lowstand (Costa et al., 2011).

A renewed expansion of lake environments occurred during the early Oligocene, its maximum expansion being represented by the coal-bearing limestones of the Calaf Fm (Fig. 8). Despite lacking direct magnetostratigraphy, the Calaf Fm grades laterally into alluvial sequences which are correlated to chron C12r (Costa et al., 2010). Sedimentation during this phase was characterized by a progressive southwards migration and retraction of lake environments (Montmaneu and Tàrraga Fms., Fig. 8). Lacustrine sedimentation was eventually interrupted after deposition of the Tàrraga Fm, when an important progradation of alluvial systems occurred.

The late Early Oligocene is characterized by a rapid westward shift of lacustrine environments to the area of Mequinenza (Fig. 1), where the MLS depocenter remained stable for the rest of the Oligocene. The basal lacustrine units of the MLS do not outcrop on surface, but their approximate limits and thickness are known from exploration boreholes (Cabrera et al., 2002). Proximal equivalents

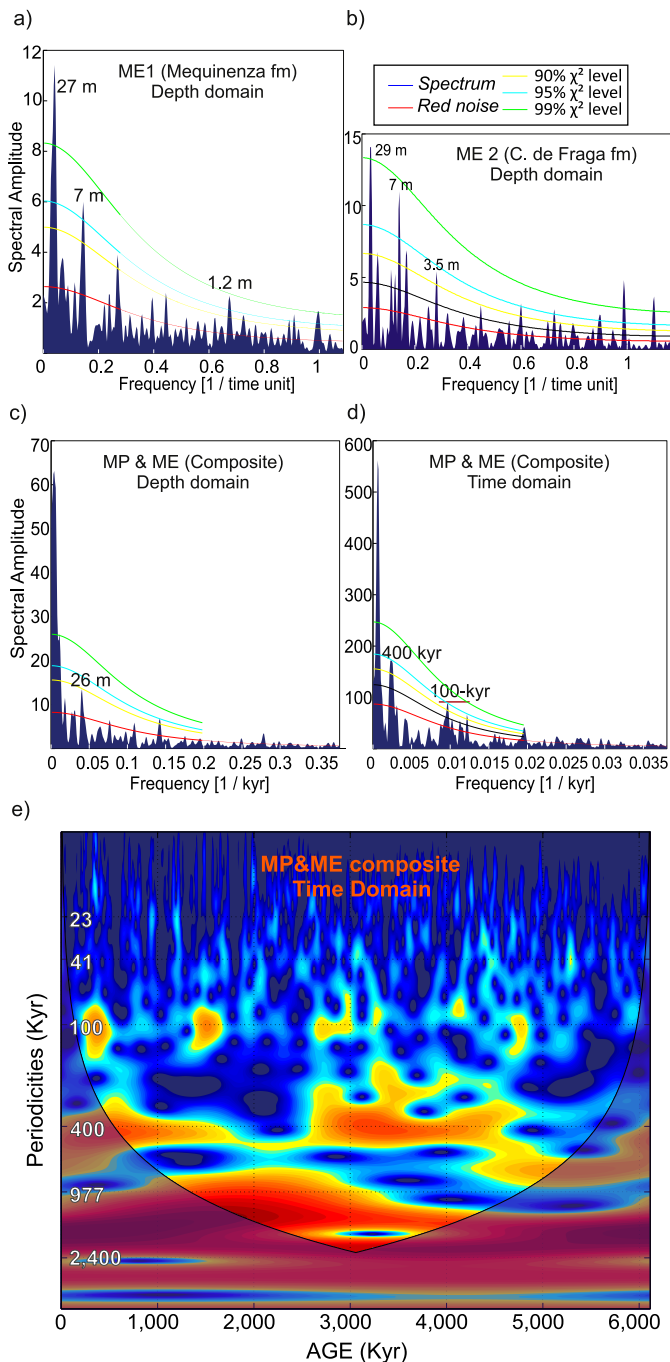


**Fig. 7.** Spectral analysis (Redfit, Schulz and Mudelsee, 2002) and wavelet analysis (Torrence and Compo, 1998) of the bathymetry time series of the MLS sequence. Spectral analysis in depth domain shows significant peaks at characteristic frequencies in each interval (A, B), while the entire section only reveals a significant peak near 26 m (C). It is interpreted that peaks at high frequencies are obscured by changes of sedimentary rates. Conversion into time domain after tuning with the 400-kyr eccentricity cycle increases notably the spectral power corresponding to the 100-kyr cycle (D). 400-kyr and 100-kyr cycles can be observed in wavelet analysis (E).

of these units are the mixed alluvial/lacustrine Marqueses Fm (Fig. 8), but its limited exposure on surface prevents further analysis on its stacking pattern.

As shown above, three major phases of lacustrine expansion were observed during the deposition of the MLS sequence. The first expansion includes the coal-bearing carbonate sequences of the lower Mequinenza Fm, dated to within chron C9n (Gomis et al., 1997). At this time, lacustrine facies spread to nearly reach

the basin margins in the Gandesa area (Barberà et al., 2001; Jones et al., 2004). The second lacustrine expansion within the Mequinenza Fm is traced along the Cinca River valley, where lacustrine limestones spread northwards over more than 10 km on top of distal alluvial red mudstones of Pyrenean source (Fig. 5). The Mequinenza depocenter experienced a sharp and temporary disappearance of lacustrine environments during the latest Oligocene, followed by a new last expansion during the earliest Miocene (Torrente de Cinca limestone Fm, Fig. 5).

After deposition of the Torrente de Cinca Fm, lacustrine environments migrated westwards to the central parts of Ebro Basin. A shallow-lake carbonate belt (Alcubierre Fm, Fig. 8) graded laterally into a thick evaporitic sequence which accumulated in the basin center since the Oligocene. First expansion of the carbonates of the Alcubierre Fm is dated in the Albalatillo section to within chron C6An.1n (Pérez-Rivarés et al., 2002). In the Sierra de Alcubierre a second cycle peaks within chron C5Dn (Pérez-Rivarés et al., 2002), followed at the Early/Middle Miocene transition by the most pronounced lake expansion of the whole record (Pérez-Rivarés et al., 2004). A sharp basin-wide transition from the salt to fresh water lake environments (Arenas and Pardo, 1999) indicates an important rise of water balance, in coincidence with the warm phase of the middle Miocene Climate Optimum (Holbourn et al., 2007).

The spatial and temporal distribution of sedimentary environments in the Ebro Basin reveals a long-term migration of lake depocenters, a process in first place controlled by the patterns of tectonic thrust sheet loading, crustal subsidence and uplift. During the Late Eocene, the location of earliest lake environments was determined by the foredeep flexure adjacent to the South-Pyrenean Front (Anadón et al., 1989). In the Early Oligocene the cratonwards shift of the flexural subsidence (Vergés et al., 2002), coupled with the progradation of the clastic wedge caused a southwards migration of the lake environments. Finally, by the late Oligocene the East Iberian margin was involved in the rifting of the western Mediterranean region (Gaspar-Escribano et al., 2004). This new geodynamic regime caused uplift in the eastern Ebro Basin and, consequently, a westward migration of the sedimentary depocenters.

In addition to the long-term migration of lacustrine depocenters, shorter wavelength oscillations in the size of lake environments occurs at a mean period of 2.4-Myr. Discerning between both is not straightforward and requires a three-dimensional view of the sedimentary stacking pattern. However, some lake expansion pulses were of such amplitude that led to their identification at distances over 100 km. Shrink and disappearance of lake environments also occurred at key intervals such as the Eocene/Oligocene and the Oligocene/Miocene transitions.

The magnetostratigraphy-based chronology of the continental Ebro Basin infill supports a correlation of periods of maximum expansion of lake environments with maxima of the 2.4 Myr eccentricity cycle, thus suggesting orbital forcing. It is noteworthy that this view challenges earlier interpretations, which associate the formation-scale stratigraphic architecture in foreland systems with tectonic processes (Alonso-Zarza et al., 2002; Miall, 2014). It is suggested that sensitivity to climate change of the lake systems in the Ebro Basin was possibly facilitated by the buffer effect of the sediment transfer systems, large enough to attenuate the supply-driven tectonic signal that propagated from active margins (Castelltort and Van Den Driessche, 2003; Armitage et al., 2013).

## 6. Eccentricity paced climates in the circum-Mediterranean area

The astronomical tuning of the MLS sequence shows that periods of lacustrine expansions are associated with times of eccentricity maxima of the 100-kyr, 400-kyr and 2.4-Myr cycle (Fig. 2),



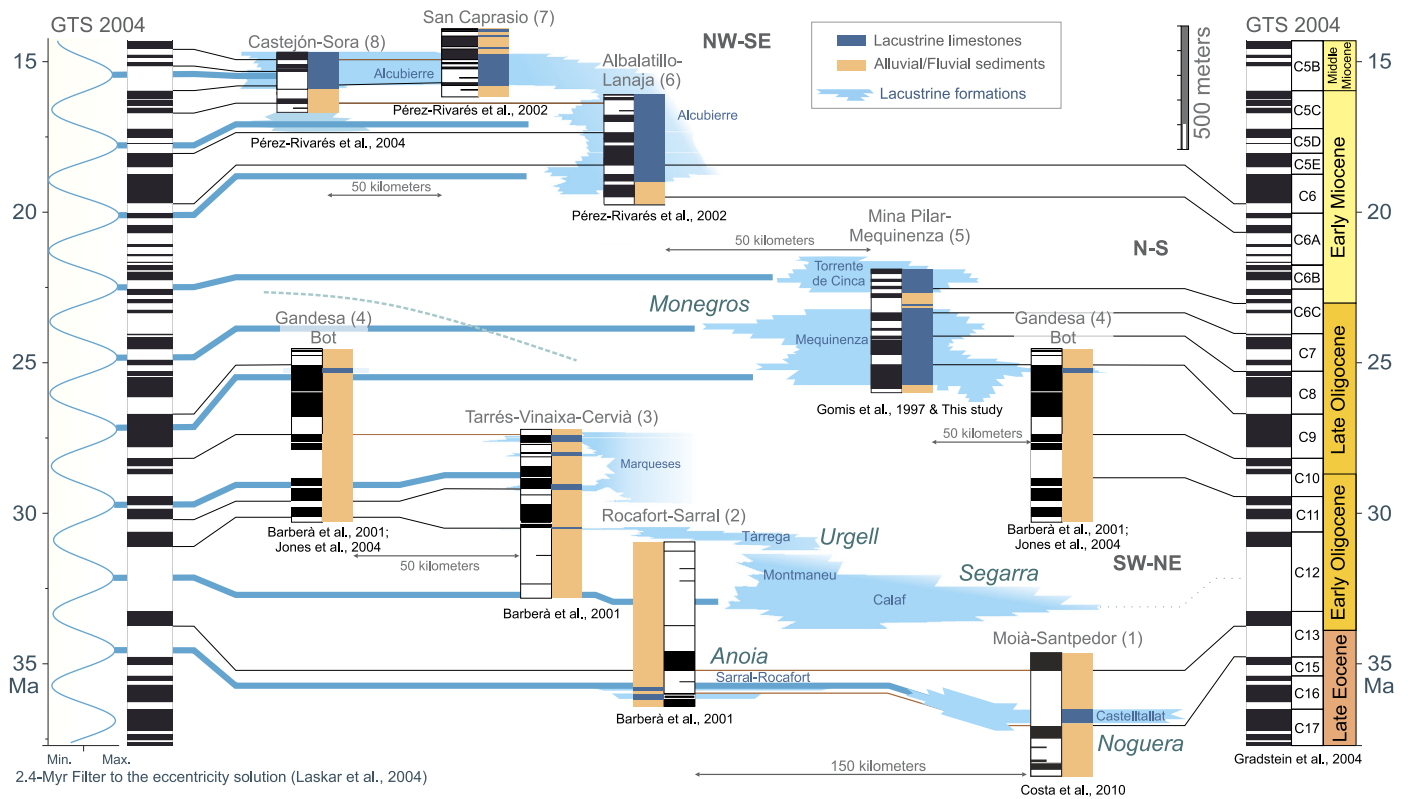


**Fig. 8.** A magnetostratigraphy-based chronostratigraphy of the continental record of the eastern (bottom panel) to central (top panel) Ebro foreland basin (see location of panels in Fig. 1). In the left, a 2.4-Myr band-pass filter of the eccentricity solution (Laskar et al., 2004) and the GPTS (Gradstein et al., 2004). Blue lines mark peaks of 2.4-Myr eccentricity maxima. In the middle, magnetostratigraphy and synthetic lithostratigraphy of key-sections (see location in Fig. 1), with indication of lacustrine (dark blue) and alluvial/fluviol sediments (brown). The lateral extent of lacustrine formations (light blue) is based on field correlations (Anadón et al., 1989; Arenas and Pardo, 1999; Barberà et al., 2001), and are faded out to mark the end of lateral control.

whereas times of eccentricity minima are marked by shrinking of lake environments. These results are in agreement with earlier studies in the Mediterranean region (Lourens et al., 2004) and other perimediterranean Neogene records (van Vugt et al., 2001; Abdul Aziz et al., 2003; Abels et al., 2009) which concluded that the 100-kyr and 400-kyr eccentricity minima and maxima were related to periods of low- and high-average precipitation respectively. Since the contribution of the 2.4-Myr cycle to the insolation spectra is very low (Laskar et al., 2004), it is inferred that long-period orbital forcing is transmitted through modulation of the shorter eccentricity cycles of 400-kyr and (specially) 100-kyr and, consequently, by the amplitude of the precession cycle. It has been suggested that an important moisture source in the northern Mediterranean borderland regions could be the North Atlantic cyclones, with prevailing southern trajectories at times of precession minima (Tuenter et al., 2004; Kutzbach et al., 2014). It is plausible then that the Iberian plate, situated along the track of the north Atlantic depressions entering the Mediterranean region, was receptive to this orbital forcing, as shown in the Pliocene sediments of the Guadalquivir Basin (Sierra et al., 2000).

The continuous record of sapropels in the Mediterranean basin suggests that coupling between precession and atmospheric circulation predicted for recent times extended into the Miocene (Tuenter et al., 2004; Abels et al., 2009; Mourik et al., 2010). Likewise, the long continuous eccentricity-paced record of wet/dry periods in the Ebro Basin suggests that a similar coupling extended into Paleogene climates of southwestern Europe. During this period, substantial paleogeographic transformations occurred, which include the progressive closing of the Atlantic-Indian connection through the Tethys Ocean, and the opening of the western Mediterranean during the Neogene. At global scale, major

changes in atmospheric and the oceanic thermohaline circulation are associated with the stepwise growth of Antarctic ice cap and Arctic glaciations (Zachos et al., 2001). It is remarkable that the imprint of long-period eccentricity cycles is not obscured by these large magnitude rearrangements, emphasizing the role of mid-latitude atmospheric circulation in Mediterranean climates.

Long-period orbital forcing related to the 2.4-Myr cycle was already pointed out in earlier studies in the Neogene continental basins of Central Spain (Abels et al., 2009, 2010; van Dam et al., 2006). However, they suggest a phase-relationship of the 2.4-Myr cycle which is opposite to our results from the Ebro basin. Particularly intriguing is the small mammal record, showing abundance of wet-adapted assemblages at times of 2.4-Myr and 0.97-Myr eccentricity minima (van Dam et al., 2006). In the Madrid Basin, the occurrence of carbonate intervals at times of 2.4-Myr eccentricity minima was attributed to a prolonged absence of relatively dry and evaporative conditions during eccentricity minima (Abels et al., 2010). But, it must be noted that carbonate formations in the Neogene basins of Central Spain basins often formed from amalgamation of palustrine calcrites and carbonate paleosols. These carbonate units were formed in poorly drained marginal areas, under very low terrigenous supply (Alonso-Zarza, 2003; Armenteros and Huerta, 2006), not necessarily linked to wetter climate conditions. On the other hand, the role that local factors (basin shape and size, relief and drainage area) exert in the link between climate and sedimentation needs to be considered. Further research is required to constrain the basin characteristics that influence the evaporation/precipitation ratios and control the diverse sedimentary responses to orbital forcing.

## 7. Conclusions

The stratigraphic architecture of the late stages (Late Eocene to Middle Miocene) of the eastern Ebro Basin shows a punctuated migration of the lacustrine systems as a response to the balance between sediment supply and subsidence (Fig. 1). Superposed to this trend of shifting depocenters, the periodic expansion and retraction of the successive lake units indicates that orbital forcing is expressed over a wide range of frequencies, included the million-year scale. Spectral analysis reveals significant power at 100-kyr and 400-kyr linked to the short- and long-eccentricity cycles. In addition, a magnetostratigraphic framework which embraces a 20 Myr long record has allowed identifying very-long period oscillations of the lake system associated to the 2.4-Myr eccentricity cycle.

Despite the important paleogeographic rearrangements in the Mediterranean region and the high-amplitude global climate shifts during the Oligocene and Miocene, lake environments remained paced by the orbital eccentricity. Times of lake expansion representing relatively wet periods are correlated to eccentricity maxima. This is a phase-relationship which is shared with most of Neogene Mediterranean basins.

It is worth noting that these conclusions are reached in the context of a foreland basin, where million-year scale sedimentary sequences are often interpreted as of tectonic origin. Discerning between long-period orbital cycles and tectonic-driven sequences is revealed as a fundamental issue in interpreting the large-scale stratigraphic architecture in foreland systems. A decoupling between tectonically-forced clastic sequences and climate-forced lacustrine sequences arises as a plausible scenario.

## Acknowledgements

This research was funded by the Spanish project COFORSED (CGL2010-17479) and the Research Group of “Geodinàmica i Anàlisi de Conques” (2009GGR 1198). LV acknowledges the University of Barcelona for financial support (APIF-UB). We thank Bet Beamud and Núria Carrera for paleomagnetic sampling assistance. Thanks to the Laboratory of Paleomagnetism of Barcelona (CCiTUB-ICTJA CSIC). This is a contribution to the ESF Research Networking programme EARTHTIME-EU. Hemmo Abels and two anonymous reviewers are thanked for their thorough reviews that contributed to improve the manuscript. Sébastien Castelltort is thanked for a previous revision of the manuscript.

## Appendix A. Supplementary material

Supplementary material related to this article can be found online at <http://dx.doi.org/10.1016/j.epsl.2014.10.007>.

## References

- Abdul Aziz, H., Krijgsman, W., Hilgen, F., Wilson, D., Calvo, J.P., 2003. An astronomical polarity timescale for the late middle Miocene based on cyclic continental sequences. *J. Geophys. Res.* 108 (B3).
- Abels, H.A., Abdul Aziz, H., Calvo, J.P., Tuenter, E., 2009. Shallow lacustrine carbonate microfacies document orbitally paced lake-level history in the Miocene Teruel Basin (North-East Spain). *Sedimentology* 56, 399–419.
- Abels, H.A., Aziz, H.A., Krijgsman, W., Smeets, S.J.B., Hilgen, F.J., 2010. Long-period eccentricity control on sedimentary sequences in the continental Madrid Basin (middle Miocene, Spain). *Earth Planet. Sci. Lett.* 289, 220–231.
- Alonso-Zarza, A.M., 2003. Palaeoenvironmental significance of palustrine carbonates and calcretes in the geological record. *Earth-Sci. Rev.* 60, 261–298. [http://dx.doi.org/10.1016/S0012-8252\(02\)00106-X](http://dx.doi.org/10.1016/S0012-8252(02)00106-X).
- Alonso-Zarza, A.M., et al., 2002. Tertiary. In: Gibbons, W., Moreno, T. (Eds.), *The Geology of Spain*. Geological Society, London, pp. 293–334.
- Anadón, P., Cabrera, L., Coldeforns, B., Sáez, A., 1989. Los sistemas lacustres del Eoceno superior y Oligoceno del sector oriental de la Cuenca del Ebro. *Acta Geol. Hisp.* 24, 205–230.
- Arenas, C., Pardo, G., 1999. Latest Oligocene–Late Miocene lacustrine systems of the north–central part of the Ebro Basin (Spain): sedimentary facies model and palaeogeographic synthesis. *Palaeogeogr. Palaeoclimatol. Palaeoecol.* 151, 127–148.
- Armenteros, I., Huerta, P., 2006. The role of clastic sediment influx in the formation of calcrete and palustrine facies: a response to paleographic and climatic conditions in the Southeastern Tertiary Duero basin (northern Spain). In: Alonso-Zarza, Eds A.M., Tanner, L.H. (Eds.), *Paleoenvironmental Record and Applications of Calcretes and Palustrine Carbonates*. In: *Spec. Pap., Geol. Soc. Am.*, vol. 416, pp. 119–132.
- Armitage, J.J., Dunkley Jones, T., Duller, R.A., Whittaker, A.C., Allen, P.A., 2013. Temporal buffering of climate-driven sediment flux cycles by transient catchment response. *Earth Planet. Sci. Lett.* 369–370, 200–210.
- Barberà, X., 1999. Magnetostratigrafia de l'Oligocè del sector sud-oriental de la Conca de l'Ebre: implicacions magnetobiocronològiques i seqüencials. PhD Thesis. Publications Univ. de Barcelona, Barcelona.
- Barberà, X., Cabrera, L., Marzo, M., Parés, J.M., Agustí, J., 2001. A complete terrestrial Oligocene magnetobiostratigraphy from the Ebro Basin, Spain. *Earth Planet. Sci. Lett.* 187, 1–16.
- Cabrera, L., 1983. Estratigrafia y Sedimentología de las formaciones lacustres del tránsito Oligoceno–Mioceno del SE de la cuenca del Ebro. PhD Thesis. Univ. de Barcelona, Barcelona.
- Cabrera, L., Sáez, A., 1987. Coal deposition in carbonate-rich shallow lacustrine systems: the Calaf and Mequinenza sequences (Oligocene, eastern Ebro Basin, NE Spain). *J. Geol. Soc.* 144, 451–461.
- Cabrera, L., Cabrera, M., Gorchs, R., de las Heras, F.X., 2002. Lacustrine basin dynamics and organosulphur compound origin in a carbonate-rich lacustrine system (Late Oligocene Mequinenza Formation, SE Ebro Basin, NE Spain). *Sediment. Geol.* 148, 289–317.
- Cande, S.C., Kent, D.V., 1995. Revised calibration of the geomagnetic polarity timescale for the Late Cretaceous and Cenozoic. *J. Geophys. Res.* 100, 6093–6095.
- Castelltort, S., van Den Driessche, J., 2003. How plausible are high-frequency sediment supply-driven cycles in the stratigraphic record? *Sediment. Geol.* 157, 3–13.
- Costa, E., Garcés, M., López-Blanco, M., Beamud, E., Gómez-Paccard, M., Larrasoaña, J.C., 2010. Closing and continentalization of the South Pyrenean foreland basin (NE Spain): magnetochronological constraints. *Basin Res.* 22, 904–917.
- Costa, E., Garcés, M., Sáez, A., Cabrera, L., López-Blanco, M., 2011. The age of the “Grande Coupure” mammal turnover: new constraints from the Eocene–Oligocene record of the Eastern Ebro Basin (NE Spain). *Palaeogeogr. Palaeoclimatol. Palaeoecol.* 301, 97–107.
- van Dam, J.A., Abdul Aziz, H., Alvarez Sierra, M.A., Hilgen, F.J., van den Hoek Ostende, L.W., Lourens, L.J., Mein, P., van der Meulen, A.J., Pelaez-Campomanes, P., 2006. Long-period astronomical forcing of mammal turnover. *Nature* 443, 687–691.
- DeCelles, P.G., Giles, K.A., 1996. Foreland basin systems. *Basin Res.* 8, 105–123.
- Freytet, P., Plaziat, J.C., 1982. Continental carbonate sedimentation and pedogenesis–Late Cretaceous and Early Tertiary of southern France. In: Purser, B.H. (Ed.), *Contrib. to Sedimentology*, vol. 12. Schweizerbart'sche Verlag, Stuttgart, 217 pp.
- García-Castellanos, D., Vergés, J., Gaspar-Escribano, J., Cloetingh, S., 2003. Interplay between tectonics, climate, and fluvial transport during the Cenozoic evolution of the Ebro Basin (NE Iberia). *J. Geophys. Res.* 108, B7.
- Gaspar-Escribano, J., García-Castellanos, D., Roca, E., Cloetingh, S., 2004. Cenozoic vertical motions of the Catalan Coastal Ranges (NE Spain): the role of tectonics, isostasy and surface transport. *Tectonics* 23 (1).
- Gomis, E., Parés, J.M., Cabrera, L., 1997. Nuevos datos magnetostratigráficos del tránsito Oligoceno–Mioceno en el sector SE de la Cuenca del Ebro (provincias de Lleida, Zaragoza y Huesca, NE de España). *Acta Geol. Hisp.* 32, 185–199.
- Gradstein, F.M., Ogg, J.G., Smith, A.G., 2004. *A Geologic Time Scale 2004*. Cambridge University Press, Cambridge, UK.
- Gradstein, F.M., Ogg, J.G., Schmitz, M., Ogg, G., 2012. *The Geologic Time Scale 2012 2-Volume Set*. Elsevier.
- Holbourn, A., Kuhnt, W., Schulz, M., Flores, J.-A., Andersen, N., 2007. Orbitally-paced climate evolution during the middle Miocene “Monterey” carbon–isotope excursion. *Earth Planet. Sci. Lett.* 261, 534–550.
- Jones, M.A., Heller, P.L., Roca, E., Garcés, M., Cabrera, L., 2004. Time lag of syntectonic sedimentation across an alluvial basin: theory and example from the Ebro Basin, Spain. *Basin Res.* 16, 467–488.
- Kashiwaya, K., Ochiai, S., Sakai, H., Kawai, T., 2001. Orbit-related long-term climate cycles revealed in a 12-Myr continental record from Lake Baikal. *Nature* 410, 71–73.
- Kirschvink, J.L., 1980. The least-squares line and plane and the analysis of palaeomagnetic data. *Geophys. J. Int.* 62, 699–718.
- Kutzbach, J.E., Chen, G., Cheng, H., Edwards, R.L., Liu, Z., 2014. Potential role of winter rainfall in explaining increased moisture in the Mediterranean and Middle East during periods of maximum orbitally-forced insolation seasonality. *Clim. Dyn.* 42 (3–4), 1079–1095. <http://dx.doi.org/10.1007/s00382-013-1692-1>.
- Lanci, L., Parés, J.M., Channell, J.E.T., Kent, D.V., 2005. Oligocene magnetostratigraphy from Equatorial Pacific sediments (ODP Sites 1218 and 1219, Leg 199). *Earth Planet. Sci. Lett.* 237, 617–634.

- Laskar, J., Robutel, P., Joutel, F., Gastineau, M., Correia, A.C.M., Levrard, B., 2004. A long-term numerical solution for the insolation. *Astron. Astrophys.* 285, 261–285.
- Liebrand, D., Lourens, L.J., Hodell, D.A., de Boer, B., van de Wal, R.S.W., Pälike, H., 2011. Antarctic ice sheet and oceanographic response to eccentricity forcing during the early Miocene. *Clim. Past* 7, 869–880.
- Lourens, L., Hilgen, F., 1997. Long-periodic variations in the earth's obliquity and their relation to third-order eustatic cycles and late Neogene glaciations. *Quat. Int.* 40, 43–52.
- Lourens, L.J., Hilgen, F.J., Shackleton, N.J., Laskar, J., Wilson, D.S., 2004. The Neogene Period. In: Gradstein, F.M., Ogg, J.G., Smith, A. (Eds.), *A Geologic Time Scale 2004*. Cambridge University Press, Cambridge, pp. 405–440.
- Luzón, A., González, A., Muñoz, A., Sánchez-Valverde, B., 2002. Upper Oligocene–Lower Miocene shallowing-upward lacustrine sequences controlled by periodic and non-periodic processes (Ebro Basin, northeastern Spain). *J. Paleolimnol.* 28, 441–456.
- Machlus, M.L., Olsen, P.E., Christie-Blick, N., Hemming, S.R., 2008. Spectral analysis of the lower Eocene Wilkins Peak Member, Green River Formation, Wyoming: support for Milankovitch cyclicity. *Earth Planet. Sci. Lett.* 268, 64–75.
- Miall, A.D., 2014. *Fluvial Depositional Systems*. Springer, New York, USA.
- Mourik, A.A., Bijkerk, J.F., Cascella, A., Hüsing, S.K., Hilgen, F.J., Lourens, L.J., Turco, E., 2010. Astronomical tuning of the La Vedova High Cliff section (Ancona, Italy) – implications of the Middle Miocene climate transition for Mediterranean sapropel formation. *Earth Planet. Sci. Lett.* 297, 249–261.
- Olsen, P.E., 1986. A 40-million-year lake record of early Mesozoic orbital climatic forcing. *Science* 234, 842–848.
- Olsen, P.E., Kent, D.V., 1996. Milankovitch climate forcing in the tropics of Pangaea during the Late Triassic. *Palaeogeogr. Palaeoclimatol. Palaeoecol.* 122, 1–26.
- Olsen, P.E., Kent, D.V., 1999. Long-period Milankovitch cycles from the Late Triassic and Early Jurassic of eastern North America and their implications for the calibration of the Early Mesozoic time-scale and the long-term behaviour of the planets. *Philos. Trans. Math. Phys. Eng. Sci.* 357, 1761–1786.
- Paillard, D., Labeyrie, L., Yiou, P., 1996. Macintosh program performs time-series analysis. *Eos Trans. AGU* 77, 379.
- Pälike, H., Norris, R.D., Herrle, J.O., Wilson, P.A., Coxall, H.K., Lear, C.H., Shackleton, N.J., Tripathi, A.K., Wade, B.S., 2006. The heartbeat of the Oligocene climate system. *Science* 314, 1894–1898.
- Paola, C., Heller, P.L., Angevine, C.L., 1992. The large-scale dynamics of grain size variation in alluvial basins, 1: theory. *Basin Res.* 4, 73–90.
- Pérez-Rivarés, F., Garcés, M., Arenas, C., Pardo, G., 2002. Magnetocronología de la sucesión miocena de la Sierra de Alcubierre (sector central de la cuenca del Ebro). *Rev. Soc. Geol. Esp.* 15, 217–231.
- Pérez-Rivarés, F., Garcés, M., Arenas, C., Pardo, G., 2004. Magnetostratigraphy of the Miocene continental deposits of the Montes de Castejón (central Ebro basin, Spain): geochronological and paleoenvironmental implications. *Geol. Acta* 2, 221–234.
- Petersen, K.D., Nielsen, S.B., Clausen, O.R., Stephenson, R., Gerya, T., 2010. Small-scale mantle convection produces stratigraphic sequences in sedimentary basins. *Science* 329, 827–830.
- Sáez, A., Anadón, P., Herrero, M.J., Moscariello, A., 2007. Variable style of transition between Palaeogene fluvial fan and lacustrine systems, southern Pyrenean foreland, NE Spain. *Sedimentology* 54, 367–390.
- Schulz, M., Mudelsee, M., 2002. REDFIT: estimating red-noise spectra directly from unevenly spaced paleoclimatic time series. *Comput. Geosci.* 28, 421–426.
- Shackleton, N.J., Crowhurst, S.J., Weedon, G.P., Laskar, J., 1999. Astronomical calibration of Oligocene–Miocene time. *Philos. Trans. Math. Phys. Eng. Sci.* 357, 1907–1929.
- Sierro, F.J., Ledesma, S., Flores, J.A., Torrecusa, S., Martínez del Olmo, W., 2000. Sonic and gamma-ray astrochronology: cycle to cycle calibration of Atlantic climatic records to Mediterranean sapropels and astronomical oscillations. *Geology* 4, 695–698.
- Torrence, C., Compo, G.P., 1998. A practical guide to wavelet analysis. *Bull. Am. Meteorol. Soc.* 79, 61–78.
- Tuenter, E., Weber, S.L., Hilgen, F.J., Lourens, L.J., Ganopolski, A., 2004. Simulation of climate phase lags in response to precession and obliquity forcing and the role of vegetation. *Clim. Dyn.* 24, 279–295.
- Vergés, J., Fernández, M., Martínez, A., 2002. The Pyrenean orogen: pre-, syn-, and post-collisional evolution. *J. Virtual Explorer* 8, 57–76.
- van Vugt, N., Langereis, C.G., Hilgen, F.J., 2001. Orbital forcing in Pliocene–Pleistocene Mediterranean lacustrine deposits: dominant expression of eccentricity versus precession. *Palaeogeogr. Palaeoclimatol. Palaeoecol.* 172, 193–205.
- Zachos, J., Pagani, M., Sloan, L., Thomas, E., Billups, K., 2001. Trends, rhythms, and aberrations in global climate 65 Ma to present. *Science* 292, 686–693.